CARBON 60 (2013) 41–45

Available at www.sciencedirect.com

SciVerse ScienceDirect

journal homepage: www.elsevier.com/locate/carbon

How the shape of catalyst nanoparticles determines their crystallographic orientation during carbon nanofiber growth

I.A. Merkulov [a,b,c], Mina Yoon [b,*], David B. Geohegan [b]

[a] Department of Materials Science and Engineering, University of Tennessee, Knoxville, TN 37996-2200, USA
[b] Center for Nanophase Materials Sciences, Oak Ridge National Laboratory, Oak Ridge, TN 37831, USA
[c] A.F. Ioffe Physico-Technical Institute RAS, 26 Politehnicheskaia str., St. Petersburg 19021, Russia

ARTICLE INFO

Article history:
Received 15 November 2012
Accepted 26 March 2013
Available online 6 April 2013

ABSTRACT

A theoretical model is presented that explains spontaneous changes in the crystalline orientation of nanoparticles. The spontaneous changes in crystalline orientation are attributed to the crystal anisotropy of the surface energy of nanocrystalline particles. We consider an important specific case of the chemical vapor deposition growth of carbon nanofibers, where previous studies have shown that both the catalyst nanoparticle shape and the nanofiber growth rate change with changes in the chemical potential of diluted carbon. Energetic considerations of the nanoparticle's free surface and its interfacial energy with the nanofiber during these shape changes are shown to force a reorientation of the nanoparticle crystallographic axes at a critical growth rate. The model therefore reveals the mechanism by which the shape and crystallographic orientation of the catalyst nanoparticle are linked to the nanofiber growth rate. The model suggests a new way, based upon measurable geometry of nanoparticles during *in situ* growth experiments, to estimate the role of chemisorption in the attraction of the graphene film to the curved catalyst surface and the anisotropy energy of this interface.

Published by Elsevier Ltd.

1. Introduction

One of the surprising properties of crystalline metal nanoparticles is the fact that below the melting temperature they have a crystalline lattice (as a solid body), however they can appear to change shape simultaneously like a viscous fluid [1,2]. It has long been observed in real-time environmental transmission electron microscopy experiments that crystalline catalyst particles change their shape during the chemical vapor deposition (CVD) growth of carbon nanofibers [3] and carbon nanotubes [4–8]. In the experiments, a correlation between the CVD growth rate and the orientation of the catalyst nanoparticle's crystalline axis was detected [9]. For some critical growth rate (v_{cr}), the value of which depends upon catalyst nanoparticle volume, the cross section of the catalyst in the direction perpendicular to growth direction changed symmetry.

In the present paper we show that this correlation follows from a general property of nanocrystals – the anisotropy of surface energy with angle. The reorientation of the nanoparticle's crystal axes with its changing shape is an inverse effect to the normal understanding that the shape of a macroscopic crystalline particle directly results from its crystalline orientation. During growth, the orientation of a nanoparticle's crystalline axes results from the correlation between the shape of a catalytic nanoparticle, the chemical potential of carbon diluted in the catalyst, and the nanofiber growth rate [10]. The equations obtained below make it possible to estimate an important parameter of the catalyst/nanofiber system – the relationship between the anisotropy energy for the free

* *Corresponding author.* Fax: +1 865 576 6885.
E-mail address: myoon@ornl.gov (M. Yoon).
0008-6223/$ - see front matter Published by Elsevier Ltd.
http://dx.doi.org/10.1016/j.carbon.2013.03.054

catalyst surface area and for the interface between the catalyst and nanofiber. This parameter not only governs the aforementioned nanoparticle axes orientation, but also gives qualitative information about the mechanism of chemical attraction between the graphene film and the nanoparticle surface.

2. Theoretical modeling of catalyst nanoparticles during the CVD growth of nanofibers

2.1. Surface energy of nanoparticles and interface energies

Most theoretical studies consider a catalyst particle as a completely crystalline object at zero temperature (T) [11–13], where any structural change is essentially prohibited. On the other hand, nanofiber synthesis is conducted at high temperatures, where the center of the catalytic particle remains crystalline, while the surface atoms freely evolves [1,2,4–8]. As experimentally observed during the nanotube growth conditions (which is very similar to that of nanofibers) this thin layer involving the precipitation of the carbon at the crystalline metal nanoparticle interface involves atomistic descriptions of defects, vacancies, and steps which introduce a state of disorder [4–8]. Therefore, under actual experimental conditions, a catalyst nanoparticle can minimize its surface energy and change its shape at the same time.

Let us consider the energy density of the free catalyst surface. In zero approximation the catalyst particle can be described as a spherical body neglecting its shape anisotropy. In this case, the surface energy density is defined as $\gamma_{f,0}$. We consider the next order and introduce the surface anisotropy of the crystalline nanoparticle by introducing the anisotropy parameter A_f, which vanishes if the macroscopic crystal temperature is higher than the melting temperature T_m. This parameter is multiplied on the cubic invariant, created from the unit perpendicular to surface vector $\mathbf{n}$[1] [14]:

$$\gamma_f \approx \gamma_{f,0} + A_f(n_x^4 + n_y^4 + n_z^4) + O(n^6) \quad (1)$$

where n_x, n_y, n_z, defined along the crystals axis, are the components of $\boldsymbol{n}$. A similar formula for the interface energy density (γ_I) can be written in terms of the energy density of the spherical interface ($\gamma_{I,0}$) and the interface anisotropy parameter (A_I). The surface and interface energies/energy densities depend not only on the nanoparticle's shape but also on its crystalline orientation. Therefore, the nanoparticle shape determines the energetically preferred orientation of the crystal axes.

Fig. 1 presents our model system of a catalyst nanoparticle on top of a carbon nanofiber. In zero approximation (assuming spherical symmetry of the catalyst material) the whole system has cylindrical symmetry. In this case, the ratio of the surface energy of the free catalyst surface and the interface are connected with the angles α and β characterizing the system. α is the angle between the free catalyst and the graphite surfaces and β is the angle between the interface and the graphite surfaces. The ratio between the energy densities is [10]:

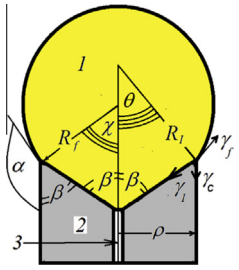

Fig. 1 – Schematic of catalyst particle (1) atop a growing nanofiber (2) of radius ρ which has a hollow orifice (3) in its center. R_f and R_I are the of curvature radii of the free catalyst surface area and interface (on its perimeter). $\beta + \theta = \pi/2$. The balance of forces of surface tension on the perimeter of interface is possible, if $\alpha + \beta > \pi$; $\chi + \beta > \pi/2$. Thus $\chi \geqslant \theta$. Tension forces, which act on the small element of the interface perimeter from the catalyst and carbon free surfaces and interface are proportional to $\gamma_f, \gamma_C, \gamma_I$. For growth steady state regime they create a forces triangle [10].

$$\gamma_f : \gamma_I(\zeta) : \gamma_C = (-\sin(\alpha+\beta)) : \sin(\alpha) : \sin(\beta) \quad (2)$$

where γ_f is the energy density of free catalyst surface, γ_C the energy density of nanofiber surface, and γ_I the interface energy density. The renormalized value γ_I depends on the chemical potential of carbon (ζ) dissolved in the catalyst. Consequently the correlation between the catalyst shape and the growth rate ($\mathbf{v}(\zeta)$) appears. This correlation results in a connection between the growth rate and the orientation of the catalyst nanoparticle's crystalline axes which has been detected in experiments [9].

2.2. Changes in shape and crystalline orientation of the catalyst particles

Fig. 2 illustrates the connections between physical processes responsible for the changes in shape and crystalline orientation of the catalyst particles during CVD growth. The chemical potential (ζ) of carbon in the catalyst particle not only determines the nanofiber growth rate (v), but also determines the interface energy (γ_I) between the catalyst particle and the nanofiber. As shown in Eq. (2) and Fig. 1, this interface energy governs the shape of the catalyst nanoparticle. At a certain carbon chemical potential, ζ_{cr} (and catalyst shape) the crystal anisotropy of the surface energy of the nanocrystalline particles will result in an energy advantage for the nanoparticle to spontaneously reorient its crystallographic axes. Thus, the experimentally-observed dynamics between the catalyst nanoparticle shape, crystallographic orientation, and nanofiber growth rate are linked.

In the following we will show that the measurable critical angles corresponding to the axes reorientation allow one to determine the anisotropy parameters for the catalyst and the interface.

Let us examine how the anisotropy of the catalyst surface changes with the growth rate of the nanofibers. In the first

[1] The 4th order of the surface vector components is the first non-vanishing term; the 1st, 2nd and the 3rd orders are vanished due to crystal cubic symmetry.

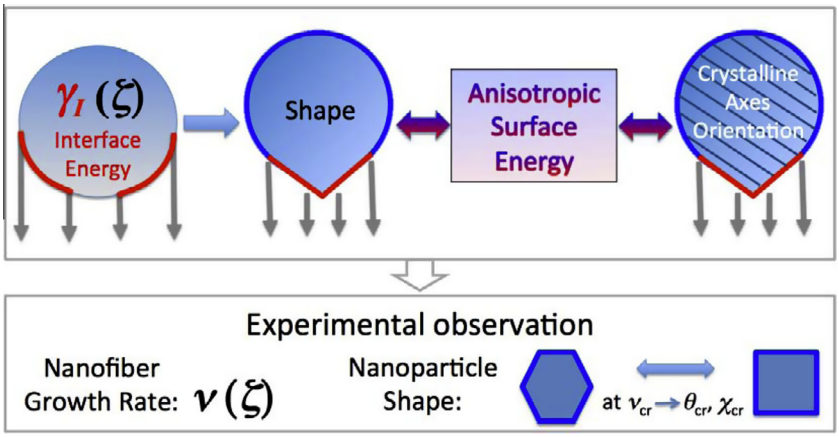

Fig. 2 – Diagram illustrating the physical processes responsible for the shape changes and the reorientation of catalyst nanoparticle crystalline axes that have been observed experimentally with changing carbon nanofiber growth rate. The chemical potential (ζ) of carbon in the catalyst particle not only determines the nanofiber growth rate (v), but also determines the interface energy (γ_I) between the catalyst particle and the nanofiber. This interface energy governs the shape of the catalyst nanoparticle. The crystal anisotropy of the surface energy of the nanocrystalline particles drives the orientation of their crystallographic axes. Thus, the shape and crystallographic orientation of catalyst nanoparticles are governed by the interface energy with the carbon.

approximation of introducing the anisotropy we write down energies of the catalyst free surface ($E_f(\mathbf{v})$) and interface ($E_I(\mathbf{v})$) derived from the energy densities (Eq. (1)) as:

$$E_m(\mathbf{v}) \approx E_{m,0}(\mathbf{v}) + B_m(\mathbf{v})[e_x^4 + e_y^4 + e_z^4] \tag{3}$$

where $E_{m,0}$ ($\mathbf{v}$) and B_m ($\mathbf{v}$) are spherical energy and anisotropy energy for each, $\mathbf{e} = \mathbf{v}/v$ is a unit vector along the growth direction, and x, y, and z are the crystallographic axes of the catalyst of index $m = f$, I (f for catalyst free surface and I for interface). In the zero approximation we treat the catalyst particle as a cylindrically symmetric object [10] and find the relationship between the energies $E_{m,0}(\mathbf{v})$, $B_m(\mathbf{v})$ and the angles β and χ (Fig. 1). Here we introduce angle χ defining the spherical segment of the catalyst.

Let us consider a small segment of the spherical catalyst surface of radius R in the angle interval $(\theta, \theta + d\theta)$. and apply the energy density in Eq. (1) to obtain a finite element of energy (dE) of such surface. By integrating Eq. (1) over the segment surface we obtain the energy of the segment (dE) as:

$$dE \approx -\left[\left(\gamma_0 + A\left(\frac{3}{8} + \frac{9}{4}t^2 - \frac{21}{8}t^4\right)\right) + A\left(\frac{3}{8} - \frac{15}{4}t^2 + \frac{35}{8}t^4\right)\right] \times 2\pi R(t)^2 dt \tag{4}$$

here γ_0 is the surface energy, A is the anisotropy parameter, t is defined as $t \equiv \cos(\theta) = (\mathbf{n} \cdot \mathbf{e})$, a scalar product of the vector normal to the interface ($\mathbf{n} = \mathbf{R}/R$) and the vector parallel to the nanofiber growth direction ($\mathbf{e}$), and $\theta = \pi/2 - \beta$. The total surface energy is obtained by integrating Eq. (4) over the angle θ of the given catalyst nanoparticle.

Next we apply the above general formalism to a catalyst/nanofiber system with a geometry defined by Fig. 1. In this case, the nanoparticle's interface has practically a conical shape[2] and its free surface is a part of a sphere [10]. We further simplify the problem and consider a large-volume catalyst particle, where ρ is large enough so that the small unstable interface region (highlighted as region three in Fig. 1, orifice of the nanofiber [15,16]) can be neglected. By applying and integrating Eq. (4) to the spherical portion of the catalyst the total energies read:

$$E_{f,0} = \left[\gamma_{f,0}(1 + \cos\chi) + A_f\left(\frac{3}{5} + \cos\chi\left(\frac{3}{8} + \frac{3}{4}\cos^2\chi - \frac{21}{40}\cos^4\chi\right)\right)\right] \times 2\pi R_f^2 \tag{5}$$

$$B_f = \cos\chi\left(\frac{3}{8} - \frac{5}{4}\cos^2\chi + \frac{7}{8}\cos^4\chi\right)2\pi R_f^2 A_f \tag{6}$$

where R_f is the radius of the spherical part of the particle. As the angle χ approaches 180°, the surface area becomes smaller and finally, at $\chi = 180°$, both $E_{f,0}$ and B_f terms vanish. As χ approaches 0°, on the other hand, $E_{f,0}$ closes to $(2\gamma_f + 6A_f/5)2\pi R_f^2$ and the B_f term vanishes due to spherical symmetry of surface. The remaining part of the catalyst particle has a conical interface and the total energies for the region become:

$$E_{I,0}(\theta) = \left(\gamma_i + A_I\left(\frac{3}{8} + \frac{9}{4}\cos^2\theta - \frac{21}{8}\cos^4\theta\right)\right)\frac{\pi\rho^2}{\cos\theta} \tag{7}$$

$$B_I(\theta) = A_I\left(\frac{3}{8} - \frac{15}{4}\cos^2\theta + \frac{35}{8}\cos^4\theta\right)\frac{\pi\rho^2}{\cos\theta} \tag{8}$$

We have to mention here that radii R_f, ρ, and angles χ, θ are not the independent parameters of the system. They are connected through the equation for catalyst volume $3V = \pi[R_f^3(2 + 3\cos\chi - 2\cos^3\chi) + \rho^3\tan\theta]$. Therefore, for fixed catalyst volume Eqs. (5) and (6) are not valid in the limit of $\theta \to \pi/2$, where the nanofiber radius gets close to the radius of the orifice, and one cannot neglect the orifice region in

[2] For element of the conical surface one should change in Eq. (4), $2\pi R(t)^2 dt$ on $\pi(d\rho^2)/\cos\theta$.

calculations. As $\theta \to 0$ $E_{I,0}$, and B_I become $\gamma_I \pi \rho^2$ and $A_I \pi \rho^2$, respectively and the conical surface degenerates into the plane, perpendicular to the growth direction ($\mathbf{n} \| \mathbf{e}$).

2.3. Critical angles and experimental observables

Finally, the entire catalyst on the nanofiber consists of the spherical and conical parts, thus the total energy becomes the sum of the energies from each region. The total energy of the crystal lattice orientation anisotropy is a linear combination of Eqs. (6) and (7), i.e. $B_\Sigma = B_f(\chi) + B_I(\theta)$. $R_f \sin\chi$ is equal to ρ and in developing the equation for B_Σ it is convenient to consider ρ^2 and A_I (or A_f) as common factors. The surface energy anisotropy changes sign depending on the coefficient of the each term, A_f/A_I and χ, θ[3] For the positive orientation anisotropy energy, i.e. $B_\Sigma(\chi, \theta; A_f, A_I) > 0$, the most favorable growth direction is the [111] crystal axis and accordingly, the catalyst cross section transverse to the growth direction has a hexagonal symmetry. On the other hand, for $B_\Sigma(\chi, \theta; A_f, A_I) < 0$, the most favorable growth direction becomes the [100] crystal axis, with the catalyst cross section of a square symmetry. Here we identify critical parameters (v_{cr}, χ_{cr}, θ_{cr}) at which the symmetry of the catalyst cross section changes with respect to the growth rate. Those parameters satisfy the condition, $B_\Sigma(\chi = \chi_{cr}, \theta = \theta_{cr}; A_f/A_I) = 0$. By solving the equation we find the connection between the experimentally measured angles and the relation of the anisotropy of the free catalyst surface area and interface. It follows:

$$A_f/A_I = f(\theta_{cr})/g(\chi_{cr}) \tag{9}$$

where,

$$f(\theta_{cr}) = \left[3 - 30\cos^2\theta_{cr} + 35\cos^4\theta_{cr}\right]/(8\cos\theta_{cr}) \tag{10}$$

$$g(\chi_{cr}) = \cos\chi_{cr}(10\cos^2\chi_{cr} - 3 - 7\cos^4\chi_{cr})/(4\sin^2\chi_{cr}) \tag{11}$$

These functions depend only on the critical angles (see Fig. 3). Both functions have solutions at which their values vanish. The solutions are $\theta_{cr,1} \approx 31^\circ$, $\theta_{cr,2} \approx 70^\circ$, $\chi_{cr,1} \approx 49^\circ$, which means that A_f/A_I can essentially have any real values. Physically it means that the critical point may exist for arbitrary A_f/A_I. For high nanofiber growth rates the angles approach 90° ($\chi, \theta \to \pi/2$) [10]. Therefore, as the growth rate increases from low values with both angles are smaller than $\chi_{cr,1} \approx 49^\circ$ to high values one will inevitably reach a critical growth rate v_{cr}, where dramatic changes will be observed in the orientation of the catalyst nanoparticle axes and the shape of the catalyst cross section. As shown in Fig. 3, measuring the critical values of the angles $\theta_{cr} = \theta_A$, $\chi_{cr} = \chi_B$ at this moment will specify $f(\theta_A)$ and $g(\chi_B)$ to allow, through Eq. (9), the estimation of A_f/A_i which essentially contains all the information about the anisotropy of the carbon nanofiber interaction to the catalyst surface.

This experimental measure of the anisotropy energy of this interface may prove very useful to understand the character of metal–graphene interactions, specifically their strength and nature (van der Waals vs chemisorption). Recent

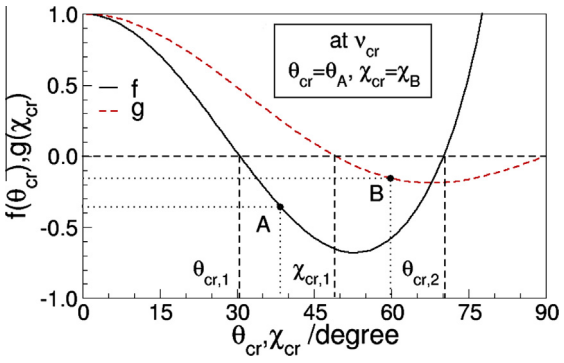

Fig. 3 – Functions *f* (black solid line) and *g* (red dashed line) from Eqs. (10) and (11), plotted for the critical angles θ_{cr} and χ_{cr} which correspond to the particle geometry (refer to Fig. 1) where the orientation of the crystalline axes of the catalyst nanoparticle, as well as its cross-sectional shape, undergo a spontaneous transition. At a critical growth rate, v_{cr}, experimental measurement of the critical angles (e.g., θ_A and χ_B) will allow determination of points *A* and *B*, from which the anisotropy ratio $A_f/A_I = f(\theta_A)/g(\chi_B)$ can be determined. (For interpretation of the references to colour in this figure legend, the reader is referred to the web version of this article.)

studies have demonstrated that the strength of graphene interactions with metal substrates change significantly for different metals [17]. However, it is theoretically and experimentally still very challenging to precisely calculate or measure these interface interactions for different crystalline [17,18,19].[4] Like multilayer graphene, carbon nanofibers are composed of multilayered and curved graphitic carbons where individual layers are principally bound to each other by weak dispersion interactions (van der Waals forces) as compared to chemical interactions. For typical nanofiber diameters (~10 or 100 nm) curvature can be neglected and, to a good approximation therefore, chemical interactions between the nanofiber and the catalyst surface originate from the inner-most carbon layer of the nanofiber that is in direct contact with the metal surface. Thus, the strength and nature of different metal–graphene interactions may be inferred from the experimental measure of interfacial anisotropy energy in carbon nanofiber growth.

3. Conclusion

In summary, we conclude a general phenomenon unique to nanoscale particles that their shape determines the preferred orientation of their crystalline axes. This is the inverse effect to the well-known determination of macroscopic crystal shapes that are governed by their crystalline orientations. Such reorientation of crystalline axes of nanoparticle behavior has been detected in different experiments. Here we considered the specific case of the CVD growth of carbon

[3] It follows from the existence of the $(\gamma_f, \gamma_I, \gamma_C)$ force triangle that $\chi \geqslant \theta$.

[4] For the case when conical approximation for interface is not valid this estimation may be done numerically on the base of the general Eq. (5).

nanofibers, where it is well known that both the catalyst nanoparticle shape and the nanofiber growth rate change with changes in the chemical potential of diluted carbon. We conclude, from energetic considerations of the nanoparticle's free surface and its interfacial energy with the nanofiber, that these shape changes force a reorientation of the nanoparticle crystallographic axes at a critical nanofiber growth rate. Thus we unveil the mechanism by which the shape and crystallographic orientation of the catalyst nanoparticle are linked to the nanofiber growth rate in accordance with experimental observations [9]. Furthermore our model offers insights into the nanofiber CVD growth processes and suggests a new experimental way to estimate the role of chemisorption in the attraction of the graphene film to the curved catalyst surface and the anisotropy energy of this interface.

Acknowledgements

We would like to thank A.V. Melechko for fruitful discussions. Synthesis science (M.Y., D.G.) supported by the Materials Sciences and Engineering Division, Office of Basic Energy Sciences, U.S. Department of Energy. General theory of nanoparticle energetics (I.M., M.Y.) supported by theme research at the Center for Nanophase Materials Sciences, which is sponsored at Oak Ridge National Laboratory by the Scientific User Facilities Division, Office of Basic Energy Sciences, U.S. Department of Energy.

REFERENCES

[1] Strandburg KJ. Two-dimensional melting. Rev Mod Phys 1988;60(1):161–207.
[2] Tartaglino U, Zykova-Timan T, Ercolessi F, Tosatti E. Melting and nonmelting of solid surfaces and nanosystems. Phys Rep 2005;411(5):291–321.
[3] Helveg S, Lopez-Cartes C, Sehested J, Hansen PL, Clausen BS, Rostrup-Nielsen JR, et al. Atomic-scale imaging of carbon nanofibre growth. Nature 2004;427(6973):426–9.
[4] Begtrup GE, Gannett W, Meyer JC, Yuzvinsky TD, Ertekin E, Grossman JC, et al. Facets of nanotube synthesis: high-resolution transmission electron microscopy study and density functional theory calculations. Phys Rev B 2009;79(20):205409-1–6.
[5] Lin M, Tan JPY, Boothroyd C, Loh KP, Tok ES, Foo YL. Dynamical observation of bamboo-like carbon nanotube growth. Nano Lett 2007;7(8):2234–8.
[6] Koziol KKK, Ducati C, Windle AH. Carbon nanotubes with catalyst controlled chiral angle. Chem Mater 2010;22(17):4904–11.
[7] Pigos E, Penev ES, Ribas MA, Sharma R, Yakobson BI, Harutyunyan AR. Carbon nanotube nucleation driven by catalyst morphology dynamics. ACS Nano 2011;5(12):10096–101.
[8] Moors M, Amara H, de Bocarme TV, Bichara C, Ducastelle F, Kruse N, et al. Early stages in the nucleation process of carbon nanotubes. Acs Nano 2009;3(3):511–6.
[9] Melechko AV, Klein KL, Fowlkes JD, Hensley DK, Merkulov IA, McKnight TE, et al. Control of carbon nanostructure: from nanofiber toward nanotube and back. J Appl Phys 2007;102(7):074314-1–7.
[10] Merkulov IA, Klein KL, Simpson ML. A synergetic description of carbon nanofiber growth. J Appl Phys 2009;105(6):064305-1–8.
[11] Wen YN, Zhang HM. surface energy calculation of the fcc metals by using the MAEAM. Solid State Commun 2007;144(3–4):163–7.
[12] Foiles SM, Baskes MI, Daw MS. Embedded-atom-method functions for the fcc metals Cu, Ag, Au, Ni, Pd, Pt, and their alloys. Phys Rev B 1986;33(12):7983–91.
[13] Johnson RA. Analytic nearest-neighbor model for fcc metals. Phys Rev B 1988;37(8):3924–31.
[14] Landau LD, Lifshitz EM, Pitaevski LP. Electrodynamics of continuous media. Course of theoretical physics. Elsevier; 2004.
[15] Merkulov IA, Melechko AV, Wells JC, Cui H, Merkulov VI, Simpson ML, et al. Two growth modes of graphitic carbon nanofibers with herring-bone structure. Phys Rev B 2005;72(4):045409-1–7.
[16] Merkulov IA, Merkulov VI, Melechko AV, Klein KL, Lowndes DH, Simpson ML. Model of carbon nanofiber internal structure formation and instability of catalytic growth interface. Phys Rev B 2007;76(1):014109-1–8.
[17] Vanin M, Mortensen JJ, Kelkkanen AK, Garcia-Lastra JM, Thygesen KS, Jacobsen KW. Graphene on metals: a van der Waals density functional study. Phys Rev B 2010;81(8):081408-1–4.
[18] Kozlov SM, Vines F, Gorling A. Bonding mechanisms of graphene on metal surfaces. J Phys Chem C 2012;116(13):7360–6.
[19] Zhao W, Kozlov SM, Hofert O, Gotterbarm K, Lorenz MPA, Vines F, et al. Graphene on Ni(111): coexistence of different surface structures. J Phys Chem Lett 2011;2(7):759–64.